

Reprinted from

JOURNAL
OF THE
PHYSICAL
SOCIETY
OF
JAPAN



■ FULL PAPER

Electronic States of Metal Ions Incorporated in Mn-DNA

Mai NAGATORI, Masaya OJIMA, Yoriko IBUKI,
Hirokazu SAKAMOTO, and Kenji MIZOGUCHI

J. Phys. Soc. Jpn. **80** (2011) 114803

Electronic States of Metal Ions Incorporated in Mn-DNA

Mai NAGATORI, Masaya OJIMA, Yoriko IBUKI, Hirokazu SAKAMOTO, and Kenji MIZOGUCHI*

Department of Physics, Tokyo Metropolitan University, Hachioji, Tokyo 192-0397, Japan

(Received July 8, 2011; accepted August 15, 2011; published online October 12, 2011)

It is known that DNA forms compounds with a variety of divalent metal ions, which are located between the bases of a base pair, and that the net charge transfer from the metal ions to DNA occurs only in the Fe-DNA case. However, the electronic states of the metal ions have not been well established, so far. The findings of this study suggest that the water molecules within the DNA double helix play an important role for the exchange coupling between the neighboring Mn ions and that the electronic states of the Mn ions in Mn-DNA are highly ionic on the basis of the Mn hyperfine splitting parameters in solution ESR spectra. The present result should be highly helpful in further investigation of engineering DNA so that it can be used for nanowires.

KEYWORDS: DNA, divalent metal, electronic states, ESR, hyperfine splitting

1. Introduction

The physical properties of natural DNA have attracted wide interest in recent years because of scientific curiosity and potential applications to self-assembled nanostructures, such as nanowires for nanoelectronics.^{1–11} The controversial results for the electronic properties have indicated that the DNA is insulating,⁷ semiconducting,^{3,5,8,10} metallic,^{1,6,9,11} and superconducting induced by the proximity effect.⁶ Such diversity is likely to result from uncontrolled experimental conditions, such as the presence of salt residues, electron bombardment by an electron microscope, and effective doping.¹² The present consensus is that natural DNA is semiconducting with a large energy gap of more than 4 eV.¹³

Some efforts on introducing charge carriers into the base π -band have been reported. One such study involved the insertion of a divalent metal ion between the bases of each complementary base pair of the double helix, adenine–thymine or guanine–cytosine, by replacing hydrogen bonds and two Na^+ ions. The structure of DNA incorporated with metal ions has been proposed on the basis of the disappearance of proton NMR signals for the hydrogen bonds in the base pairs, as shown in Fig. 1.¹⁴ The resulting DNA structure is called M-DNA, where M is the metal ion.^{8,13–22} Rakitin *et al.* reported that Zn-DNA has ohmic current–voltage (I – V) characteristics, which is in sharp contrast to natural DNA.¹⁶ However, it has been confirmed that M-DNA with $M = \text{Zn}$, Ca , Mg , or Mn does not carry the paramagnetism accompanying charge carrier injection, suggesting no charge injection to DNA.^{8,13,18} This fact means that a simple ion exchange by the divalent metal ion for the two sodium ions in Na-DNA has occurred, keeping the electronic states of the DNA backbone unchanged. Very recently, however, Omerzu *et al.* have reported a new sample preparation technique, which provides ESR spectra typical of strongly correlated electron systems.²³ This finding contradicts the reported results obtained by a conventional sample preparation technique,¹⁸ suggesting that the electronic states of M-DNA are not unique and that they depend on the sample preparation conditions. Although several theoretical approaches to obtaining the electronic states of M-DNA have been reported, the experimental

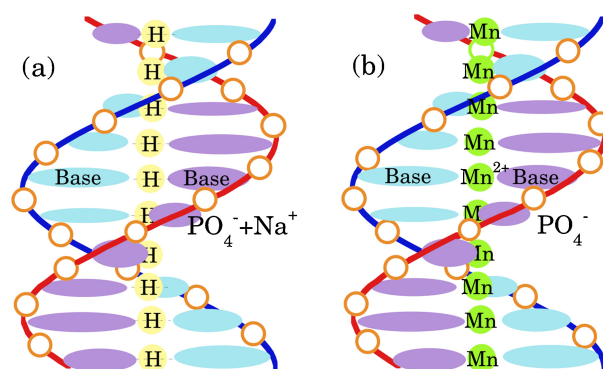


Fig. 1. (Color online) Schematic structures of (a) DNA and (b) Mn-DNA in B-form. Each divalent metal ion is inserted between the bases of a base pair in place of hydrogen bonds.¹⁴ It is expected that the magnetic interaction between the Mn ions will be one dimensional.

results for the electronic states of the divalent metal ions are crucially important for predicting the actual properties of M-DNA.^{20,24,25} Thus, it is important to characterize the electronic states of the metal ions of M-DNA.

Mn-DNA is a prototypical system for studying the electronic states of metal ions in M-DNA; it has the spin $S = 5/2$, making it a good magnetic probe.^{8,18,19,21} Several items of experimental evidence, obtained from SQUID magnetization, ESR integrated intensity, and elemental analysis are consistent with the proposed structural model shown in Fig. 1. It has been reported that the ESR spectrum of the B-form Mn-DNA has the line shape characteristic of quasi-one-dimensional (Q1D) spin correlation, but it changes markedly to that for three-dimensional (3D) spin correlation in the A-form isomer, which is stable under dry, water-deficient condition.^{18,19,21} This behavior is driven by the isomeric structural change of DNA as a function of environmental humidity, and is also evidence for the proposed structure in Fig. 1. Note that, in the A-form Mn-DNA, some long-range magnetic ordering should result from the 3D magnetic interaction, as confirmed by the low-temperature heat capacity peak below 0.4 K.¹⁸ In contrast, the B-form Mn-DNA shows no indication of the magnetic interaction, as demonstrated by the temperature-independent ESR linewidth down to 2 K.¹⁸

*E-mail: mizoguchi@phys.se.tmu.ac.jp

In this study, we perform the ESR analysis of Mn-DNA to unveil the nature of the electronic states of metal ions in the M-DNA complexes. This information will be useful for further theoretical and experimental investigations of M-DNA.

2. Experimental

Mn-DNA is prepared from an aqueous solution of DNA (salmon or oligo-DNA), provided by Wako Pure Chemical, Hokkaido System Science, and the Ogata Materials Science Lab., with MnCl_2 at the molar ratio of DNA to MnCl_2 from 1 : 5 to 1 : 10. Here, note that MCl_3 with M^{3+} does not form an M-DNA composite. Excess cold ethanol at -20°C is poured into the transparent DNA- MnCl_2 solution, resulting in the formation of a transparent precipitate of Mn-DNA. The residual MnCl_2 is washed out thoroughly from the obtained precipitate with pure ethanol, in which DNA is insoluble. Circular dichroism (CD) spectra of the Mn-DNA solution are examined to confirm the B-form of the double-helix structure.¹⁸⁾ X-ray fluorescence analysis indicated that the ratio of phosphorus to metal is approximately 2 : 1 as expected for the proposed structure in Fig. 1. The divalent metal ion is located at the center of a base pair and compensates the charges of the two phosphoric anions in the two DNA backbones of a double helix, in place of two Na cations. ESR spectra are taken mainly at X-band. The half width at half maximum of the absorption spectrum is used as the linewidth of ESR spectra. All the samples studied in this report are of polycrystalline form.

3. Discussion

3.1 Hyperfine split spectra of Mn-DNA

X-band ESR spectra of Mn-DNA with different water contents are demonstrated in Fig. 2. One finds three different types of spectra:

- (1) the top three spectra labelled as “A-form”,
- (2) the middle spectra labelled as “B-form”, and
- (3) the bottom three spectra labelled as “Solution”.

As has been discussed in ref. 18, the line shape between Gaussian and Lorentzian, which is characteristic of one-dimensional (1D) exchange narrowing²⁶⁾ for the B-form film under a humid condition, clearly transforms into the Lorentzian line shape in the dry A-form film upon removing water molecules, which corresponds to the change from (2) to (1). There are two possible origins for the line broadening in Mn-DNA: the dipolar interaction between the neighboring Mn ions, which reaches $\sqrt{\Delta B^2} \approx 160\text{ mT}$, and the six hyperfine splitting (HFS) peaks produced by the isotropic hyperfine interaction $AS \cdot I$ with $I = 5/2$ for the Mn nucleus. The resultant line shape is controlled by the dimensionality of the exchange interaction, which averages these line broadenings out.⁸⁾ The spiral Mn arrays of the A-form Mn-DNA compose the 3D exchange network within the Mn-DNA double helix and with the neighboring Mn-DNA, from which the Lorentzian line shape resulted. Unlike the A-form, the exchange interaction is confined within the 1D linear Mn array along the center axis of the B-form double helix, giving rise to the characteristic line shape of 1D systems with shorter spectral tails than the Lorentzian case.²⁶⁾ The observed second moment of the ESR spectra reported in ref. 8 is well reproduced by the dipolar

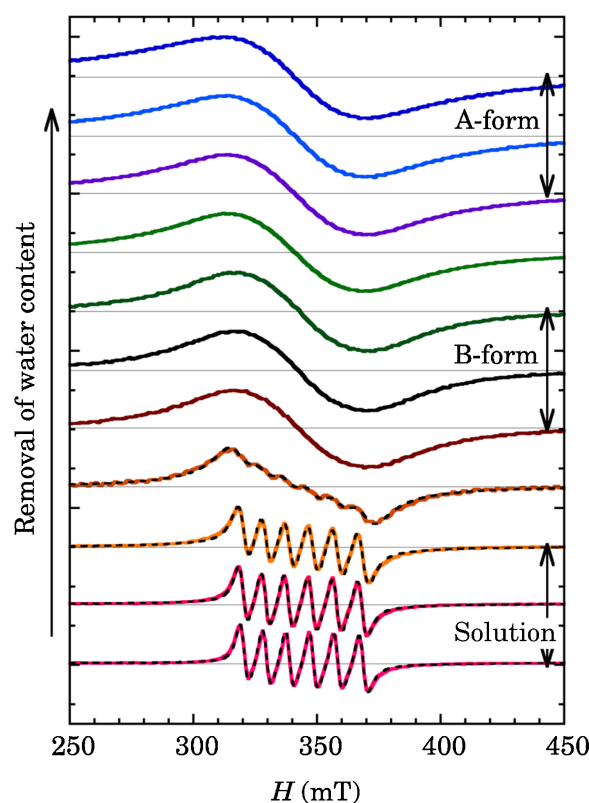


Fig. 2. (Color online) Time evolution of the ESR derivative spectra in Mn-DNA with water. By evaporating water, the spectral shape gradually changes from six hyperfine split peaks to a broad single Lorentzian shape (solid A-form state, top three spectra, $W_B = 50 \pm 3\text{ mT}$), via intermediate spectra of a 1D shape typical of the B-form Mn-DNA (fifth to seventh spectra), as discussed in ref. 18. The dashed curves represent the results of simulation with HFS + Lorentzian for the bottom four spectra. The parameters used are summarized in Table I.

interaction between Mn ions separated by the expected separation of 0.34 nm with the observed exchange interaction, which supports exclusively the model structure in Fig. 1.⁸⁾

To understand the behavior in (3), it is useful to investigate the stability of the Mn-DNA structure in Fig. 1 in an aqueous solution. Thus, we dissolved Mn-DNA in concentrated NaCl aqueous solution, where the number of Na ions exceeds the total number of Mn ions in the Mn-DNA by more than 10 times. If the Mn ions in Mn-DNA had dissolved in the surrounding NaCl solution, the counter cations for the PO_4^- anions in the two DNA backbones should have been mainly exchanged from Mn to Na in the final precipitate because of the diffusion of Mn ions into the concentrated NaCl solution. However, the magnetic properties of the Mn-DNA precipitated from the NaCl + Mn-DNA solution were unchanged. Thus, it is demonstrated that the Mn-DNA composite with the structure in Fig. 1 is highly stable even in the solution. In contrast, it is worthwhile to note that we actually obtained $\text{Ca}_{0.9}\text{Mn}_{0.1}\text{-DNA}$ from a pristine DNA solution with the molar ion ratio of one MnCl_2 to nine CaCl_2 in the initial sample preparation with pristine DNA.

The bottom three spectra with six HFS lines are obtained in the aqueous solution of Mn-DNA. The same spectra

within the experimental uncertainty are also obtained from the solutions of $(\text{Ca}_{1-x}\text{Mn}_x)\text{-DNA}$ ($x = 0.1, 0.01$). Although this type of HFS ESR spectrum is typically observed in solution, the present result is not necessarily the usual case. The HFS spectra can be observed only in isolated magnetic systems, such as diluted and isolated magnetic ions in nonmagnetic solids or solutions, where both the exchange interaction and the dipolar interaction are suppressed by isolation, in addition to the thermal molecular motion in solution. In contrast, the Mn ions in the 1D Mn array of Mn-DNA always have two nearest neighboring Mn ions at a constant distance regardless of the sample conditions, film or solution. That is, the observation of the HFS spectra in Fig. 2 implies the absence of both the exchange and dipolar interactions with the neighbors; the former erases the HFS from the spectra and the latter broadens the spectra. Since the Mn-DNA rapidly tumbles in solution, the anisotropic magnetic dipolar interaction with the surrounding Mn ions should be completely removed by motional narrowing.^{27,28} However, it is difficult to understand why the isotropic exchange interaction, which averages the HFS peaks out, is absent in the solution, because the local correlation between the neighboring Mn ions should be maintained even in the solution. This findings suggests that a certain mechanism suppresses the exchange interaction with the neighbors at a fixed distance within Mn-DNA even in the solution.

In the A-form of Mn-DNA, Lorentzian-like spectra were obtained, as demonstrated in Figs. 2 and 3.¹⁸⁾ As easily expected, it is impossible to reproduce a single Lorentzian spectrum as the simple sum of six HFS Lorentzians, as demonstrated by the broken curve in Fig. 3. This finding indicates that in the film state of the A-form Mn-DNA, the exchange interaction between the neighboring Mn ions actually averages the hyperfine splittings out, as usually expected in solids. Thus, very interestingly, the exchange interaction, which is active in the solid film of Mn-DNA, disappears in the solution, even when the local correlation in distance between the Mn ions is kept. Therefore, the issue to be solved is the mechanism for the disappearance of the exchange interaction in the Mn-DNA solution.

Here, it should be noted that the water molecules generally play an important role in DNA. In this context, there is a critical difference between the Mn-DNA solution and the film. The number of water molecules in the A-form DNA is as low as ≈ 4 , and the water molecules are spatially fixed and immobile in the major groove of DNA. In contrast, the B-form DNA in solution contains many water molecules, that is, at 93% relative humidity there are ≈ 26 water molecules per base pair,²²⁾ and the water molecules move freely in and out of the DNA. Thus, one possible mechanism for understanding the disappearance of the exchange interaction in the Mn-DNA solution is the dynamical role of the water molecules mediating the exchange coupling between the neighboring Mn ions. If the water molecules are immobile, the static exchange interaction becomes active, as in the film of Mn-DNA. However, if the water molecules can move around as in the solutions, the exchange coupling between the neighboring Mn ions is rapidly interrupted by the motion. Thus, the effective magnitude of the exchange coupling decreases with increasing interruption duration and

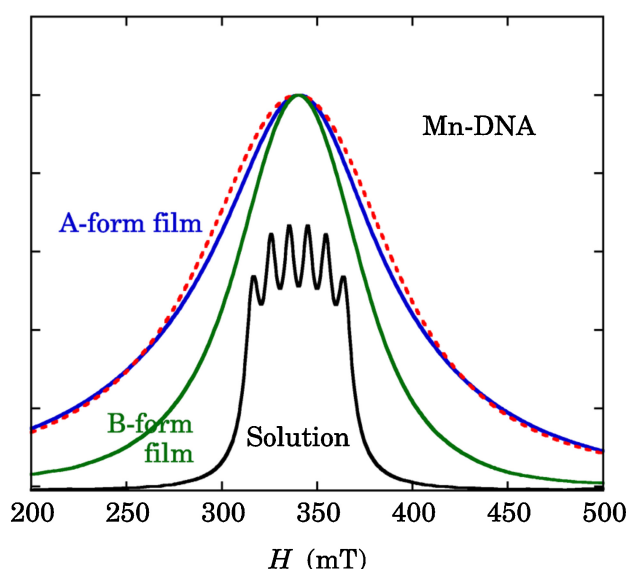


Fig. 3. (Color online) Absorption spectra for the $(\text{Ca}_{1-x}\text{Mn}_x)\text{-DNA}$ ($x = 1, 0.1, 0.01$) in solution, and B- and A-form Mn-DNA films. The spectra in solution agree with each other within the uncertainty. The simulated spectrum for the A-form Mn-DNA in terms of the six Lorentzian spectra with the same separation as those in solution Mn-DNA is also shown by the broken curve, which fails to reproduce the Lorentzian line shape in the A-form Mn-DNA.

becomes much less than that of the hyperfine interaction in the solutions. Although the detailed mechanism for the exchange coupling between the neighboring Mn ions is currently an open question, the disappearance of the effective exchange interaction in the Mn-DNA solution can be interpreted.¹⁸⁾

In relation to the exchange interaction mediated by the water molecules, it has been reported on the basis of measurements with a SQUID magnetometer that the Curie–Weiss temperature of Mn-DNA films, which is proportional to the exchange coupling constant, changes from -1 K in the B-form to -2 K in the A-form.¹⁸⁾ Here, note that the change in Curie–Weiss temperature from -1 to -2 K, which corresponds to a magnetic field strength of more than 1 T, is much larger than the HFS of <0.1 T. Under this condition, the HFS spectra of the Mn-DNA films in both the A- and B-forms should be completely averaged out by the exchange interaction between Mn ions. Also note that the average distance between the neighboring Mn ions in the A-form is similar to that in the B-form.²⁹⁾ Thus, the more than ten water molecules for each base pair in the B-form film make the effective exchange interaction small compared with that in the A-form. This observation is consistent with the Curie–Weiss temperature in the B-form Mn-DNA being smaller than that in the A-form Mn-DNA. These considerations for the exchange interaction in Mn-DNA suggest that the water molecules mediate the exchange interaction among the neighboring Mn ions, although the magnetic mechanism is an open question.

3.2 Analysis of hyperfine interaction

The hyperfine interaction between the electrons and the nucleus of a Mn ion in the unit of mT is expressed as^{27,28,30)}

Table I. Average value of the hyperfine coupling constant A_0 and the deviation A_0^2/B_0 from the equal spacing in eq. (3) in the unit of mT deduced from the simulations (expt.) for the HFS spectra of $(\text{Ca}_{1-x}\text{Mn}_x)\text{-DNA}$ solutions and the estimation (calc.) with A_0 and B_0 , along with the reference materials of $\text{Ca}(\text{Mn})\text{Cl}_2$ and $\text{Mg}(\text{Mn})\text{O}$. Experimental errors at the least significant digit are indicated in parentheses.

Unit (mT)	A_0	A_0^2/B_0	
		expt.	calc.
$(\text{Ca}_{1-x}\text{Mn}_x)\text{-DNA}$ solutions	9.62(1)	0.27(1)	0.27
$\text{Ca}(\text{Mn})\text{Cl}_2$	9.11(1)	0.24(1)	0.25
$\text{Mg}(\text{Mn})\text{O}$	8.74(1)	0.22(1)	0.22

$$\frac{\mathcal{H}_{\text{hf}}}{g\mu_B} = \mathbf{I} \cdot \mathbf{A} \cdot \mathbf{S} = A_0 \mathbf{I} \cdot \mathbf{S} + \mathbf{I} \cdot \mathbf{A}_{\text{ani}} \cdot \mathbf{S}, \quad (1)$$

where \mathbf{I} is the nuclear spin, \mathbf{S} is the electron spin, and \mathbf{A} is the hyperfine coupling tensor, which is the sum of the isotropic part A_0 and the traceless anisotropic part \mathbf{A}_{ani} . In the Mn-DNA solution, DNA double helices rapidly tumble, which averages the anisotropic part \mathbf{A}_{ani} out at zero, giving rise to $\mathbf{A} \approx A_0$. Neglecting the low nuclear Zeeman energy, the electron spin Hamiltonian for the Mn-DNA solution,

$$\frac{\mathcal{H}}{g\mu_B} \approx B_0 S_z + A_0 S_z I_z + \frac{A_0}{2} (S_+ I_- + S_- I_+), \quad (2)$$

gives the Zeeman energy for each nuclear spin multiplet m_I . The resonance condition of the HFS spectra with the Zeeman energy splittings $\Delta E(m_I)$ is given by^{28,30}

$$\frac{\Delta E(m_I)}{g\mu_B} = B_0 + A_0 m_I + \frac{1}{2} \left(\frac{A_0^2}{B_0} \right) [I(I+1) - m_I^2]. \quad (3)$$

The second term ($\propto m_I$) predicts equally spaced $2I+1=6$ peaks for $I=5/2$, which correspond to each m_I value. The third term ($\propto m_I^2$) provides a linear deviation from the equally spaced peak separation on m_I as a higher order effect of the hyperfine interaction.

The parameters deduced from the simulation with eq. (3) for $(\text{Ca}_{1-x}\text{Mn}_x)\text{-DNA}$ ($x=1, 0.1, 0.01$) solutions are summarized in Table I, along with those for the reference materials, $\text{Mg}(\text{Mn})\text{O}$ and $\text{Ca}(\text{Mn})\text{Cl}_2$ (spectra are not shown). Several characteristic features are found in this table.

- (1) The isotropic hyperfine coupling constant $A_0 = 9.62$ mT in the $(\text{Ca}_{1-x}\text{Mn}_x)\text{-DNA}$ systems is larger than both 9.11 mT in $\text{Ca}(\text{Mn})\text{Cl}_2$ and 8.74 mT in $\text{Mg}(\text{Mn})\text{O}$.
- (2) The experimentally observed deviations (expt. in Table I) from the equal separation of HFS for the $(\text{Ca}_{1-x}\text{Mn}_x)\text{-DNA}$ solutions are well reproduced by the coefficient A_0^2/B_0 in eq. (3) calculated with the experimental parameters A_0 and B_0 (calc. in Table I), suggesting that eq. (3) is a suitable expression for modeling the solution spectra.

Table II demonstrates the systematic dependence of the isotropic hyperfine coupling constant A_0 on the degree of ionicity in the bonding states of Mn^{2+} ions in the calcium halides and the chalcogenides.³¹ The bonding nature of Mn^{2+} in CaF_2 is highly ionic, but is highly covalent in CaS . In contrast, that of Mn^{2+} diluted in MgO is intermediate between the ionic and covalent bonding natures. It is possible to understand this tendency from the spatial

Table II. Hyperfine coupling constant of Mn^{2+} ions embedded in the calcium halides and chalcogenides, in the unit of mT.³¹ The linear relationship $g\mu_B A_0 = 19.4 + 83.3i$ (10^{-4} cm^{-1}) $= 2.08 + 8.92i$ (mT) has been estimated from the calculated result based on the experimental data set, where i is the degree of ionicity.³¹ Here, note that the slope depends on the host ion species. To convert mT to cm^{-1} , divide it by $1.071 \times 10^3 \text{ mT/cm}^{-1}$.

	Host			
	CaF_2	CaO	CaCl_2	CaS
A_0 (mT) for Mn^{2+}	10.1	9.18	9.11 ^{a)}	8.11
Degree of ionicity	0.90	0.80	0.79	0.68

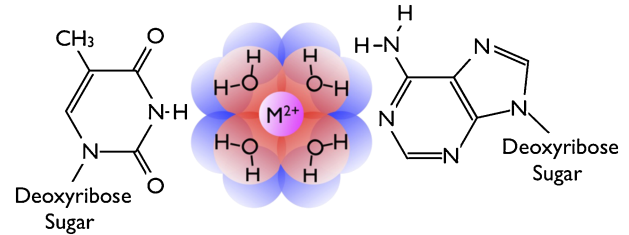


Fig. 4. (Color online) Schematic model for M-DNA. The metal ion is surrounded by several water molecules between, for example, thymine and adenine, in place of hydrogen bonds in natural DNA. This model is based on the following three points: (1) the present result of ionic bonding character, (2) the fact that metal ions preferentially form a direct covalent bond with nitrogen, and (3) the recent observations of M-DNA by STM, showing a certain ring around the metal ion between the bases. In a solution, many water molecules in addition to those in this figure fill the space around the bases and undergo a rapid exchange with each other.

distribution of $3d$ -electron wavefunctions of Mn^{2+} . Since the p or d electron has no spin density at the Mn nucleus, the isotropic interaction requires the interaction with the inner s -electron cores. Thus, the isotropic hyperfine interaction A_0 results from the polarization of the inner s -electron cores induced by the d -electron polarization (the core polarization effect).³¹ It is well known that the wavefunctions in ionic crystals are spherical and close to the isolated ions. However, the wavefunction of a covalent bonding electron tends to extend towards the bonding direction, which reduces the interaction to polarize the s -electron cores, that is, the hyperfine coupling constant. As discussed in the literature,³¹ there is a clear relationship between the hyperfine constant A_0 and the ionicity, but the magnitude of the isotropic hyperfine constant depends on the species of the host cations, such as Li, Na, K, Ca, Mg, and Zn. If one compares $A_0 = 9.6$ mT for Mn in the $(\text{Ca}_{1-x}\text{Mn}_x)\text{-DNA}$ with the average value of $A_0 = 9.8$ mT for dilute Mn substituted in several fluorides, such as LiF , NaF , KF , MgF_2 , and CaF_2 , it is reasonable to conclude that the bonding of the Mn ion in DNA is purely ionic.

Figure 4 shows the model for the Mn^{2+} ion surrounded by several water molecules between the bases of the Mn-DNA film. In a solution, many water molecules in addition to these in this figure fill the space around the bases and undergo a rapid exchange with each other. This model meets the requirement indicated by the present conclusion that metal ions should be isolated from nitrogen, since they tend to form covalent bonds. It is evident that ionic bonding negligibly modifies the electronic states of DNA. In contrast,

Omerzu *et al.* have reported that a Zn-DNA sample prepared by the new technique²³⁾ shows the Pauli-like temperature-independent behavior of ESR intensity. Their report implies the presence of a bonding nature different from the ionic one, which can sizably modify the electronic states of Zn-DNA. Unfortunately, their report²³⁾ does not indicate the type of structure and bonding electronic states of the other Zn-DNA. Therefore, further systematic investigations are required to determine the electronic states of these M-DNA systems.

4. Conclusions

The Mn^{2+} ESR study of the HFS in $(\text{Ca}_{1-x}\text{Mn}_x)$ -DNA systems has indicated the mechanism of the exchange interaction between Mn ions and the nature of the bonding state of the Mn^{2+} ions with the surrounding bases of DNA. As regards the mechanism, it is concluded that the exchange interaction between the Mn ions is mediated by water molecules, but further details remain to be obtained. As regards the bonding nature, the isotropic hyperfine coupling constant is a useful parameter, which can be deduced from the separation between the HFS peaks that correspond to the nuclear spin quantum number $m_I = \pm 1/2$. The isotropic hyperfine constant reflects the ratio of the covalent nature to the ionic nature. The observed hyperfine constant of 9.6 mT for the $(\text{Ca}_{1-x}\text{Mn}_x)$ -DNA systems is significantly larger than 8.1 mT for $\text{Ca}(\text{Mn})\text{S}$ and 9.1 mT for $\text{Ca}(\text{Mn})\text{Cl}_2$, but is close to 9.8 mT for several fluorides, such as LiF , NaF , KF , MgF_2 , and CaF_2 , with nearly perfect ionic bonding. This finding is evidence that the Mn^{2+} ions are ionically connected with the negatively charged PO_4^- ions in the two DNA backbones by Coulomb interaction via the sequence of polarizations, H_2O , and bases.

It has been determined that the Mn^{2+} ions in the present $(\text{Ca}_{1-x}\text{Mn}_x)$ -DNA systems compensate the negative charges of two PO_4^- ions in the DNA backbones, in place of two Na^+ ions. Thus, the simple exchange of two Na^+ ions with one Mn^{2+} ion should induce only a limited change of the electronic states of DNA.^{8,18,19,21)} A system in which the charges are known to transfer from the metal ions to DNA bases is Fe-DNA.^{18,19,21)} Such a system is expected to be studied systematically, along with another recently developed and very interesting system, that is, the M-DNA system with strongly correlated electrons reported by Omerzu *et al.*²³⁾ On the basis of the present conclusions, more realistic theoretical and experimental studies will be possible in the future, which will unveil the future possibility of DNA and charge-imported DNAs in nanoelectronics.

Acknowledgment

This work was supported by a Grant-in-Aid for Scientific Research on Priority Areas (17067015) from the Ministry of Education, Culture, Sports, Science and Technology and (16038220), and by Grants-in-Aid for Scientific Research C (17540334 and 17540332) from the Japan Society for the Promotion of Science.

- 1) H.-W. Fink and C. Schenkenberger: *Nature* **398** (1999) 407.
- 2) P. J. de Pablo, F. Moreno-Herrero, J. Colchero, J. Gomez Herrero, P. Herrero, A. M. Baro, P. Ordejon, J. M. Soler, and E. Artacho: *Phys. Rev. Lett.* **85** (2000) 4992.
- 3) D. Porath, A. Bezryadin, S. d. Vries, and C. Dekker: *Nature* **403** (2000) 635.
- 4) P. Tran, B. Alavi, and G. Gruner: *Phys. Rev. Lett.* **85** (2000) 1564.
- 5) K. Iguchi: *J. Phys. Soc. Jpn.* **70** (2001) 593.
- 6) A. Y. Kasumov, M. Kociak, S. Gueron, B. Reulet, V. T. Volkov, D. V. Klinov, and H. Bouchiat: *Science* **291** (2001) 280.
- 7) Y. Zhang, R. H. Austin, J. Kraeft, E. C. Cox, and N. P. Ong: *Phys. Rev. Lett.* **89** (2002) 198102.
- 8) K. Mizoguchi, S. Tanaka, T. Ogawa, N. Shiobara, and H. Sakamoto: *Phys. Rev. B* **72** (2005) 033106.
- 9) S. Nakamae, M. Cazayous, A. Sacuto, P. Monod, and H. Bouchiat: *Phys. Rev. Lett.* **94** (2005) 248102.
- 10) K. Mizoguchi, S. Tanaka, and H. Sakamoto: *Phys. Rev. Lett.* **96** (2006) 089801.
- 11) S. Nakamae, M. Cazayous, A. Sacuto, P. Monod, and H. Bouchiat: *Phys. Rev. Lett.* **96** (2006) 089802.
- 12) R. G. Endres, D. L. Cox, and R. R. P. Singh: *Rev. Mod. Phys.* **76** (2004) 195.
- 13) A. Omerzu, D. Mihailovic, B. Anzelak, and I. Turel: *Phys. Rev. B* **75** (2007) 121103R.
- 14) J. S. Lee, L. J. P. Latimer, and R. S. Reid: *Biochem. Cell Biol.* **71** (1993) 162.
- 15) H. Kino, M. Tateno, M. Boero, J. A. Torres, T. Ohno, K. Terakura, and H. Fukuyama: *J. Phys. Soc. Jpn.* **73** (2004) 2089.
- 16) A. Rakitin, P. Aich, C. Papadopoulos, Y. Kobzar, A. S. Vedenev, J. S. Lee, and J. M. Xu: *Phys. Rev. Lett.* **86** (2001) 3670.
- 17) J. B. MacNaughton, M. V. Yablonskikh, A. H. Hunt, E. Z. Kurmaev, J. S. Lee, S. D. Wettig, and A. Moewes: *Phys. Rev. B* **74** (2006) 125101.
- 18) K. Mizoguchi, S. Tanaka, M. Ojima, S. Sano, M. Nagatori, H. Sakamoto, Y. Yonezawa, Y. Aoki, H. Sato, K. Furukawa, and T. Nakamura: *J. Phys. Soc. Jpn.* **76** (2007) 043801.
- 19) K. Mizoguchi: *Proc. SPIE* **7040** (2008) 70400Q.
- 20) S. S. Mallajosyula and S. K. Pati: *Phys. Rev. Lett.* **98** (2007) 136601.
- 21) K. Mizoguchi: *Proc. SPIE* **7765** (2010) 77650R.
- 22) H. Matsui, N. Toyota, M. Nagatori, H. Sakamoto, and K. Mizoguchi: *Phys. Rev. B* **79** (2009) 235201.
- 23) A. Omerzu, B. Anzelak, I. Turel, J. Strancar, A. Potocnik, D. Arcon, I. Arcon, D. Mihailovic, and H. Matsui: *Phys. Rev. Lett.* **104** (2010) 156804.
- 24) S. S. Alexandre, J. M. Soler, L. Seijo, and F. Zamora: *Phys. Rev. B* **73** (2006) 205112.
- 25) M. Fuentes-Cabrera, B. G. Sumpter, J. E. Sponer, J. Sponer, L. Petit, and J. C. Wells: *J. Phys. Chem. B* **111** (2007) 870.
- 26) M. J. Hennessy, C. D. McElwee, and P. M. Richards: *Phys. Rev. B* **7** (1973) 930.
- 27) A. Abragam: *The Principles of Nuclear Magnetism* (Oxford University Press, Oxford, U.K., 1961) p. 159.
- 28) A. Abragam and B. Bleaney: *Electron Paramagnetic Resonance of Transition Ions* (Clarendon Press, Oxford, U.K., 1970) p. 133.
- 29) In short, the separation between the metal ions inserted into M-DNA is mainly dominated by the rectangular structure composed of two long edges of a base pair with a metal ion and two short edges of backbone units, deoxyribose sugar + phosphate + deoxyribose sugar. The actual angle between the short edge and the long edge is around 50° for the A-form and 55° for the B-form. Thus, the separation between the metal ions is approximately invariant because of the invariance of the edge lengths. In more detail, the molecular lengths of the purine bases, guanine and adenine, are larger than those of the pyrimidine bases, thymine and cytosine. Finally, only the average separations of the A- and B-forms are similar.
- 30) W. Gordy: *Theory and Application of Electron Spin Resonance* (Wiley, New York, 1980) p. 17.
- 31) A. N. Zhitomirskii: *J. Struct. Chem.* **9** (1968) 532.